Impression creep of ABS polymers

Donyau Chiang and J. C. M. Li*
Materials Science Program, Department of Mechanical Engineering, University of Rochester, Rochester, NY 14627, USA
(Received 6 July 1993; revised 5 March 1994)

The impression creep behaviour of acrylonitrile–butadiene–styrene (ABS) polymers with various butadiene contents was investigated under punching stresses of 10–120 MPa and at temperatures from 330 to 390 K ($T_g = 376$ K). It was found that the creep resistance of the ABS polymers decreased with increasing butadiene content. The impression velocities in the steady-state region were analysed using a theory involving thermally activated processes. The temperature within the testing range had little effect on the activation shear strain volume, which increased with increasing butadiene content. The slope between the activation enthalpy and temperature increased gradually when the temperatures were below 353 K and then became steeper when the temperature approached the glass transition temperature. The activation enthalpy reached a maximum of 1050 kJ mol^{-1} at 380 K and then decreased upon further increase in temperatute. Two parallel deformation mechanisms were proposed to explain this behaviour. One is a stress activation slip process which dominates at temperatures below the glass transition temperature, and the other is a free volume assisted shear process which dominates at temperatures higher than the glass transition temperature.

(Keywords: impression creep; ABS polymers; steady-state strain)

INTRODUCTION

The impression creep technique is a sample-saving measurement method in which a small diameter cylindrical punch with a flat end is pushed against the smooth specimen surface by a constant load. The impression depth is recorded as a function of time at a certain temperature. Impression creep measurements have been successfully performed to characterize the steady-state creep properties of a variety of metals[1], alloys[2] and ionic crystals[3]. Both the stress and temperature dependences of the steady-state impression velocity are in good agreement with the corresponding parameters obtained from the conventional creep test. In this study, we will extend the application of the impression creep technique to a polymer-based composite material.

Plastic deformation of acrylonitrile–butadiene–styrene (ABS) polymers has been studied both theoretically and experimentally. Moore and Gieniewski[4] carried out constant load creep measurements on a commercial ABS polymer over the temperature range 323–363 K at stress levels of 6–17 MPa. They found that application of the time–temperature superposition principle was of limited value for temperatures below the effective glass transition temperature of the acrylonitrile–styrene component of the polymer. However, they claimed that a rate theory satisfactorily described the deformational behaviour of ABS polymers. The height of the potential energy barrier, which determines the resistance experienced by the molecular flow units slipping relative to each other, decreases as stress increases.

Bergen and Wolstenholm[5] performed stress relaxation and tensile creep measurements on several thermoplastic materials, including three kinds of ABS polymers with different acrylonitrile/butadiene/styrene ratios, a poly(vinyl chloride) and a poly(methyl methacrylate). A mechanical model with eight adjustable parameters was used to describe the relaxation curves of these polymers at one temperature and seven parameters were required to fit the creep curves at different temperatures. This analysis was based on the assumption that two relationships are valid, namely that the logarithm of the shift factor is linearly related to the stress, and that the Williams–Landel–Ferry equation is valid below the glass transition temperature.

In general, there are two deformation mechanisms for polymeric materials under tensile stress conditions: shear deformation and craze formation. Bucknall and co-workers[6,7] conducted dead load tensile creep experiments at ambient temperatures on ABS polymers with and without the addition of some volume fraction of glass beads. Based on simultaneous measurements of longitudinal and lateral strain changes in the tensile gauge length, the two components, namely shear banding and crazing, contributing to the plastic deformation of the polymers could be distinguished. The authors concluded that shear deformation predominated at the early stages of the tensile creep process and the contribution of crazing to creep deformation increased rapidly with time and stress.

All experiments on the plastic deformation of ABS polymers reported in the literature have been conducted under constant tensile load conditions at temperatures below the glass transition temperature. However, it is also of importance to examine polymer deformation under compressive stress environments and at temperatures near or above the glass transition temperature. In view of the need to understand the forming and shaping

* To whom correspondence should be addressed

0032-3861/94/19/4103–07

behaviour of polymers, the above-mentioned experiments become even more important. Hence, we carried out an impression test on ABS polymers and hoped to shed some light on the deformation processes under compression within a large temperature range.

EXPERIMENTAL

Material characteristics and test specimens

The ABS polymers with different butadiene contents used in this investigation were obtained from Dow Chemical Company. Their method of producing the ABS polymers was as follows. The ABS resins were melt compounded on a twin-screw extruder at 477 K and were compression moulded at 505 K into plaques. The conditions of moulding were 10 min of preheating, 3 min at full pressure (15.3 MPa) and 15 min of cooling under the same pressure. The pellets were predried at 353 K overnight before moulding. There were no flow aids, plasticizers or additives other than the standard low level of antioxidants in these ABS resins.

The ABS polymers are composite materials in which the rubber particles (polybutadiene) are dispersed within the brittle styrene–acrylonitrile (SAN, copolymer weight-average molecular weight $M_w = 100\,000$) matrix to toughen the material. Denoted respectively as SAN, ABS-10, ABS-17 and ABS-25, four ABS blends containing 0%, 10, 17.5 and 25% rubber by volume and a 1/1 molecular ratio of acrylonitrile to styrene were used. The glass transition temperature for all four blends was 376 ± 1.5 K, determined by using a Dupont 2100 differential scanning calorimeter under a nitrogen atmosphere at a heating rate of 10 K min^{-1}. The glass transition temperature of the ABS blends was close to that of polystyrene[8]. The density of each blend was 1.05 g cm^{-3}, regardless of butadiene content. The microstructure of ABS-17 as observed by Ni *et al.*[9] has been published elsewhere. There were two sizes of rubber particles, 0.1 and 0.4 μm, with the volume fraction of the former being 100 times that of the latter.

The materials were received in plate form with dimensions of 130 (l) × 80 (w) × 12.5 (t) mm^3. Specimen blocks were cut from the as-received plates and milled to become parallelepipeds with dimensions of 25 (l) × 15 (w) × 10 (t) mm^3. Each specimen block was further ground and polished metallurgically using 0.05 μm fine alumina powders to obtain a pair of flat surfaces. After that, each specimen block was annealed at 373 K for 3.5 h and furnace cooled down to room temperature to relieve the residual stresses from moulding and machining. Four specimen blocks with different butadiene contents were prepared for the impression creep test.

Impression creep aparatus

The impression creep measurement requires a flat-ended cylindrical punch (indenter), which is the main difference between the impression creep test and the indentation creep test. The indenter shape used in the indentation creep test is usually conical, spherical or pyramidal, so the stress decreases with increasing indentation depth (or area) under constant load in an indentation creep test. However, the applied stress is constant for an impression creep test with a flat-ended cylindrical punch under constant load, especially if the penetration depth is shallow.

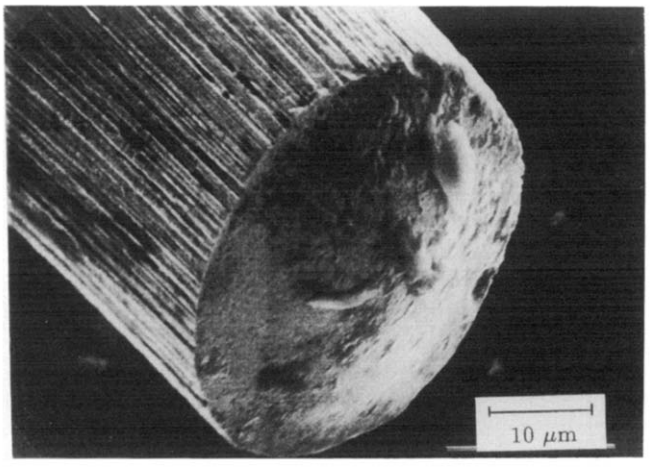

Figure 1 Scanning electron micrograph of the flattened end of the punch. The sample was tilted 35° to display the end surface

Tungsten wires of several sizes were chosen to be the punch materials. An electrochemical method was used to flatten the end of the wire. A 36% by weight sodium hydroxide solution served as the electrolyte. In this method, a piece of wire 30 mm long was cut, then attached to an aluminium plate connected to the positive terminal of a direct current power supply. A section about 5–10 mm long at the end of the wire was immersed in the electrolyte 40 mm away from the negative graphite rod. The irregular, sharp wire end resulting from the cut was rendered flat after a few minutes of electrolysis. Several careful dippings driven by a micrometer were necessary to trim the wire end finely. A typical end surface of a 50 μm diameter tungsten punch is shown in *Figure 1*, in which the sample was tilted 35° to display the flat surface. With the electrochemical technique, we made a punch as small as 25 μm in diameter. However, because of problems with the instrument alignment and environmental effects on the measuring transducers in using this small diameter punch, we only report here the impression results from the 100 μm diameter punch.

A horizontal impression creep apparatus was constructed to conduct creep measurements on the ABS materials. A schematic diagram of the set-up is shown in *Figure 2*. The tungsten punch was inserted and glued (ceramic glue) into a small ceramic tube to form a punch head. To prevent buckling during the experiment, the maximum exposed punch length was allowed to be only two to three times the wire diameter. The assembled punch head was further glued to a quartz tube through which the force could be applied.

The impression depth pushed into the specimen surface was monitored continuously as a function of time by a linear variable differential transformer (LVDT). The amount of load applied on the specimen was adjusted by either using steel balls of various weights or driving a screw vice forwards or backwards to change the loading angle. A load cell with 1 N maximum capability was carted to slide on the rail along the axial direction to monitor the force continuously. To maintain an isothermal atmosphere and reduce the temperature effects on the transducers, an insulated box with controlled heating was built to isolate the transducers from the surroundings. Two thermocouples were used in the system, one for controlling the temperature and the other for recording. The temperature fluctuations of the furnace during the

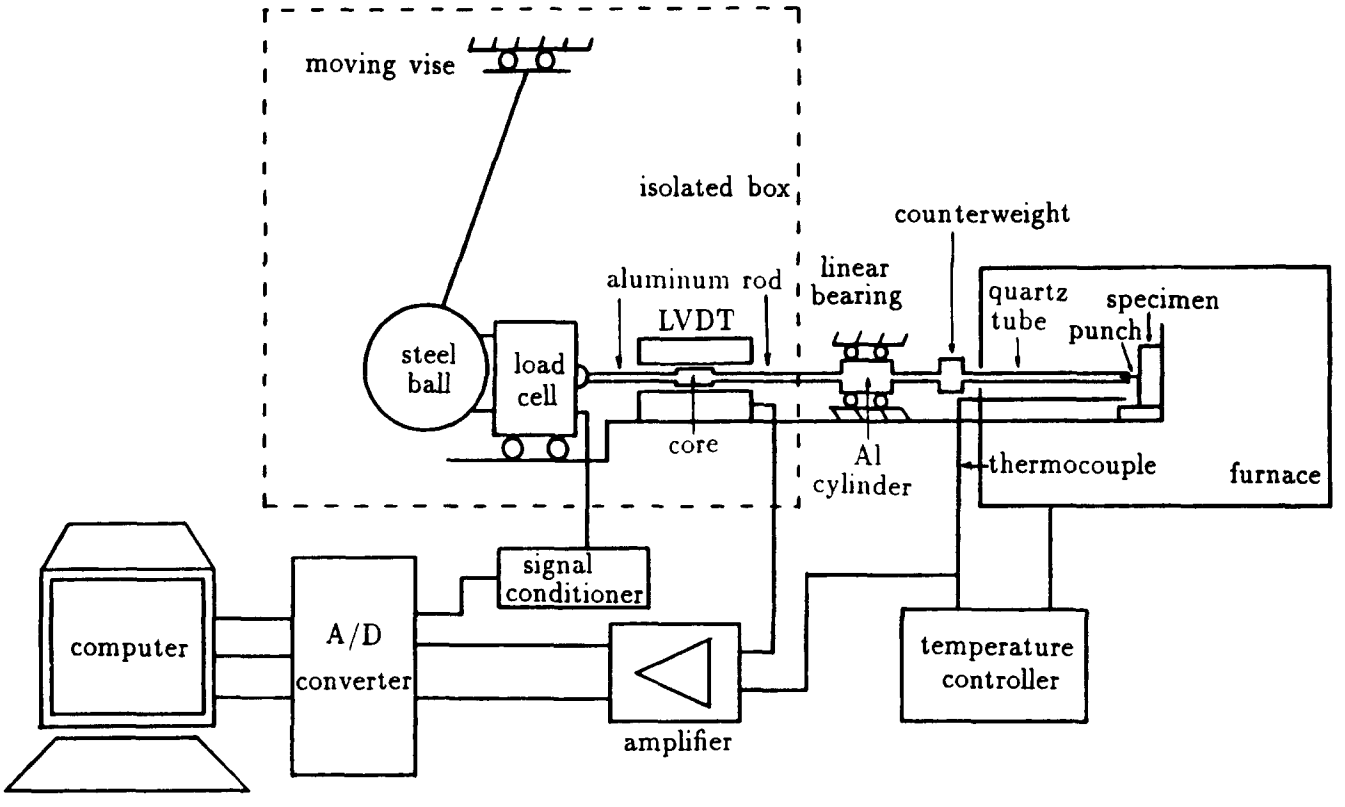

Figure 2 Schematic diagram of the horizontal impression creep apparatus

experiment were less than $\pm 0.5°C$. All experiments were performed in air.

The signals from the LVDT and the thermocouple were amplified through a differential input instrumentation amplifier with RC (resistance–capacitance) integrators. An analog–digital converter with a 10 bit capacity digitized the signals from the load cell, LVDT and thermocouple. The digitized signals were sent to an IBM PC for recording and further data processing. The maximum fluctuation in displacement measurement for this system was recorded for a day to be $\pm 0.4\,\mu m$. The resolution of the LVDT was about $0.1\,\mu m$.

Experimental procedure

The well-polished specimen was rested on a sample holder and both the specimen and the holder were put in the middle of the furnace. The furnace was heated to a predetermined temperature and it was necessary to wait for an extra hour for the sample to reach thermal equilibrium before the load was applied. The data were recorded automatically for each time period, the duration of which was set before the experiment was started. The minimum time period was 1 s. After each run the specimen was shifted to a new position and another experiment was ready to be conducted. At the beginning, the temperature was set at the lowest value. After all stress levels were examined and the stress dependence was obtained at this temperature, the experiment moved on to the next higher temperature. The purpose was to minimize the annealing effect on the specimen. By repeating these steps, all the creep information could be gathered from one specimen.

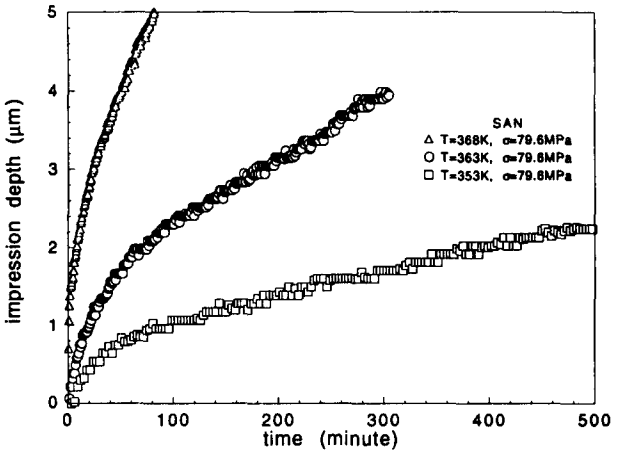

Figure 3 Impression depth *versus* time for SAN

RESULTS AND DISCUSSION

Creep curves: impression depth versus *time*

Figures 3 and *4* show the impression depth as a function of time for two ABS materials, namely SAN and ABS-25. The depth–time curves resemble the conventional creep curves with a steady-state stage following a short transient period. Because of the geometric constraints of the punch, the deformation is always stable. The transient period presumably helps to establish the steady-state plastic zone below the punch. The zone size is comparable to the punch diameter[1].

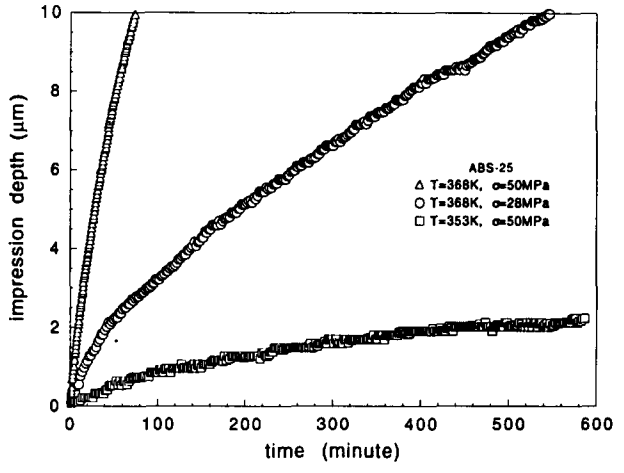

Figure 4 Impression depth *versus* time for ABS-25

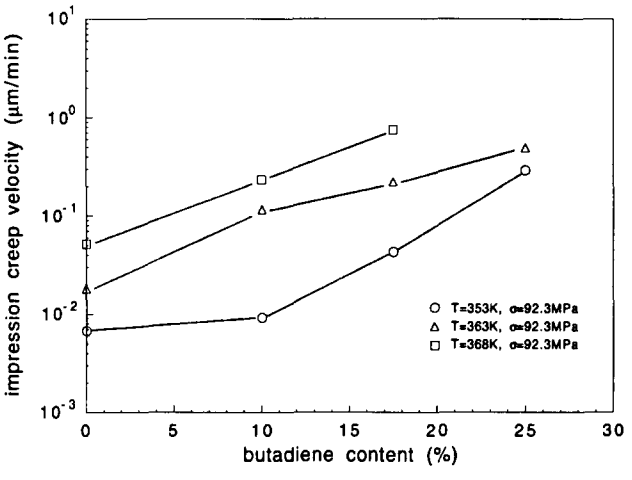

Figure 5 Effect of butadiene content on the steady-state impression velocity over the temperature range 353–368 K and a stress of 92.3 MPa

The effect of butadiene content on the steady-state impression velocity

The steady-state impression velocity (the average velocity near the end of the creep curve) increases as the butadiene content in the ABS polymer increases. The relationship, shown for three temperatures (353, 363 and 368 K) and a stress of 92.3 MPa, is illustrated in *Figure 5*. Butadiene is a soft component embedded in the hard SAN matrix to toughen the whole material. When the ABS materials are deformed under compression, the butadiene regions may act as stress concentrators, and slip is easily nucleated at these positions. The higher the butadiene content in the ABS polymer, the lower the creep resistance at elevated temperatures. Similar results have been reported in the literature[10] for rubber-toughened polypropylene, in which the addition of rubber particles accelerates the creep rate at room temperature.

Stress dependence

Figures 6–9 show the stress dependences of the steady-state impression velocities for the four ABS samples with different rubber contents. The logarithm of the steady-state impression velocity shows a linear relationship to the applied punching stress for all the materials examined under our experimental conditions, and the slopes of the lines remain similar at several temperatures. The working stress moves to a lower stress region as temperature and butadiene content increase.

The activation shear strain volume for a deformation process is defined as[11]

$$\Omega = RT\left(\frac{\partial \ln \dot{\varepsilon}}{\partial \tau}\right)_{P,T} \quad (1)$$

which may be obtained from the slope of the line at each temperature. In the equation, Ω, $\dot{\varepsilon}$ and τ are the activation

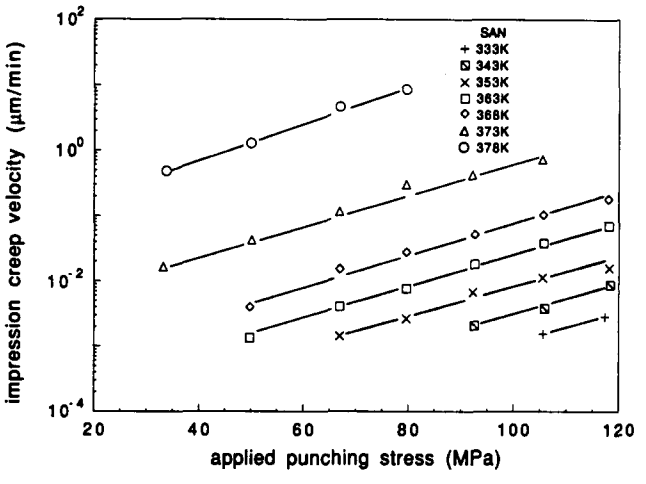

Figure 6 Stress dependence of the impression velocity for SAN

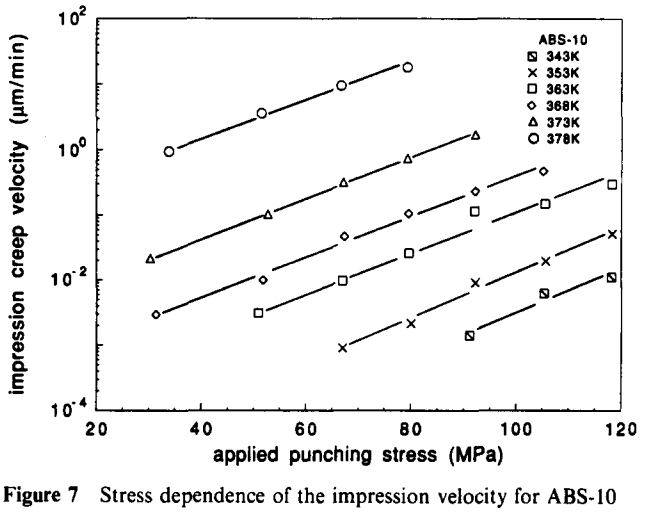

Figure 7 Stress dependence of the impression velocity for ABS-10

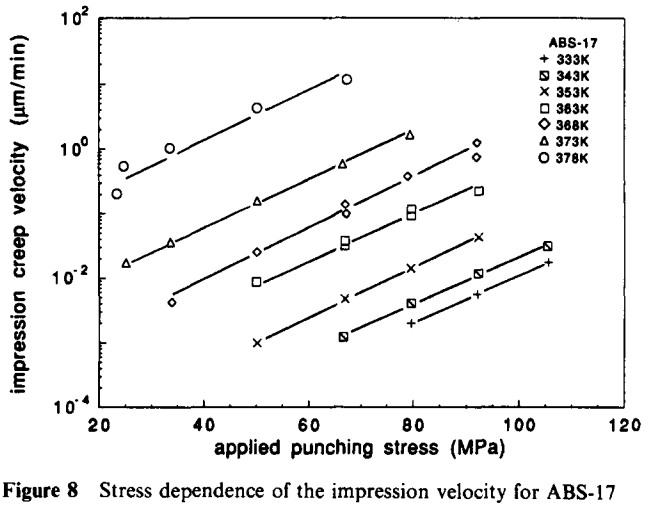

Figure 8 Stress dependence of the impression velocity for ABS-17

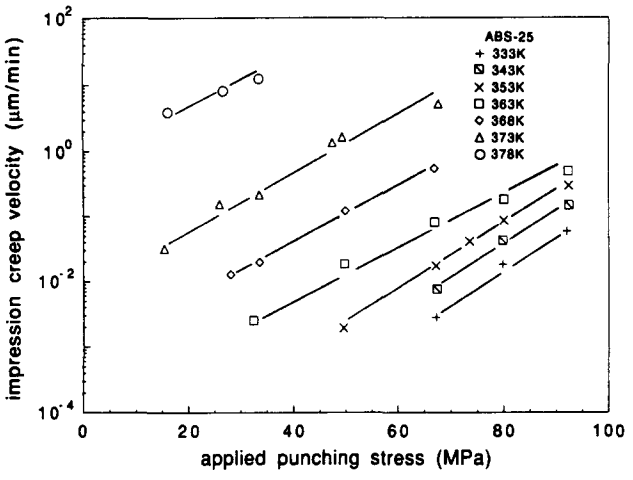

Figure 9 Stress dependence of the impression velocity for ABS-25

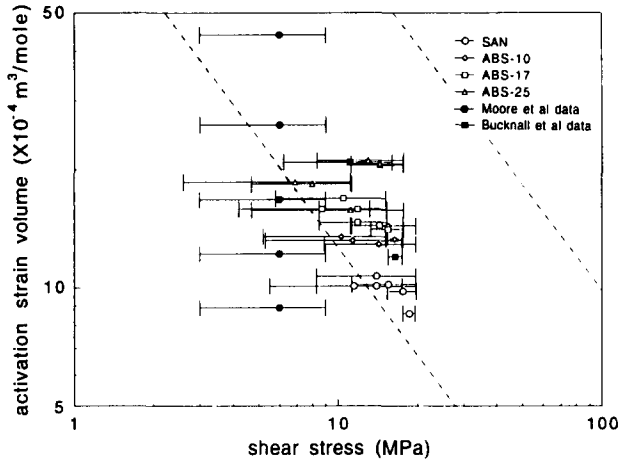

Figure 10 Double-logarithmic plot of activation shear strain volume *versus* shear stress. Each symbol is positioned at the average value of the shear stress for each temperature and the horizontal line attached to the symbol represents the stress range. Two parallel dashed lines represent the upper and lower boundaries of a general correlation for all materials[15]

shear strain volume, strain rate and shear stress, respectively. R, P and T are the gas constant, ambient pressure and absolute temperature, respectively. Because the effective shear stress instead of the punching stress and the steady-state strain rate instead of the steady-state impression velocity are required for calculation, two conversion factors are necessary. One factor transforms the punching stress to the shear stress and the other transforms the impression velocity to the strain rate. Empirically, the conversion factor for stress transformation[12,13] can be taken as 6, and the factor for velocity–strain rate transformation can be taken as the punch diameter[14]. However, since the logarithm of the strain rate is involved in equation (1), any constant multiplying the strain rate will not affect the value for the activation shear strain volume.

The double-logarithmic plot of activation shear strain volume against shear stress over the temperature range 333 K–373 K is presented in *Figure 10*. Each symbol in the figure is located at the average value of the shear stress for each temperature and the symbol has a horizontal line which expresses the stress range. Two parallel dashed lines in the plot represent the boundaries of a general correlation for all materials[15] independent of composition and temperature. The temperature seems not to have much effect on the activation shear strain volume for any given polymer, but the average activation shear strain volume increases with the butadiene content.

The data for ABS polymers of different compositions obtained in this study are near the lower boundary of the general correlation for all materials[15]. The data obtained by Bucknall and coworkers[6,7] and Moore and Gieniewski[4] are also included in the plot in *Figure 10*. Because of the tensile stresses used in their experiments, their stresses are halved to obtain the maximum shear stresses for comparison. We used the activation shear strain volume calculated at 10^4 s from the data of Moore and Gieniewski[4] and the unfilled ABS data from Bucknall and Drinkwater[6]. In general, both seem to be consistent with our data, but some of Moore and Gieniewski's data are outside the range of the general correlation.

Temperature dependence

The temperature dependences of the steady-state impression velocities (estimated near the ends of the creep curves) for the four different polymers plotted as the logarithm of impression velocity *versus* the reciprocal of absolute temperature are shown in *Figures 11–14*. The

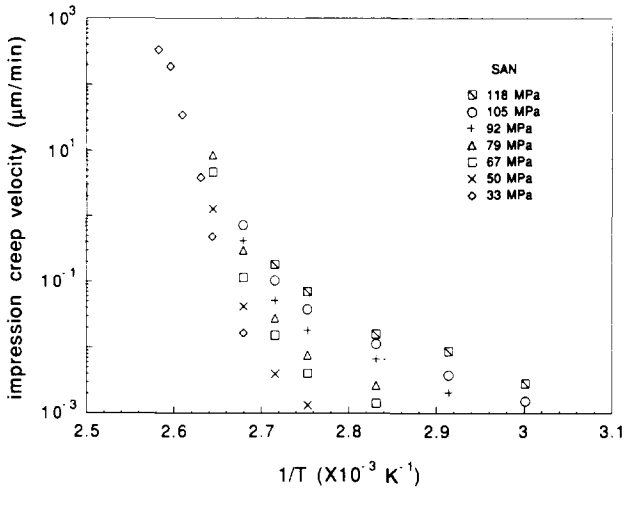

Figure 11 Temperature dependence of the impression velocity for SAN

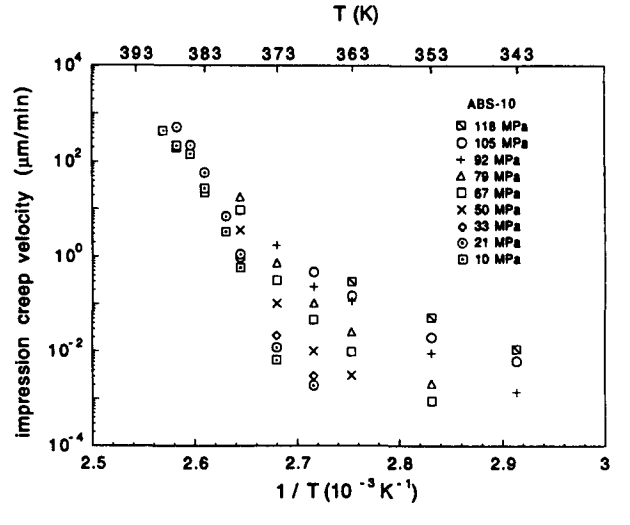

Figure 12 Temperature dependence of the impression velocity for ABS-10

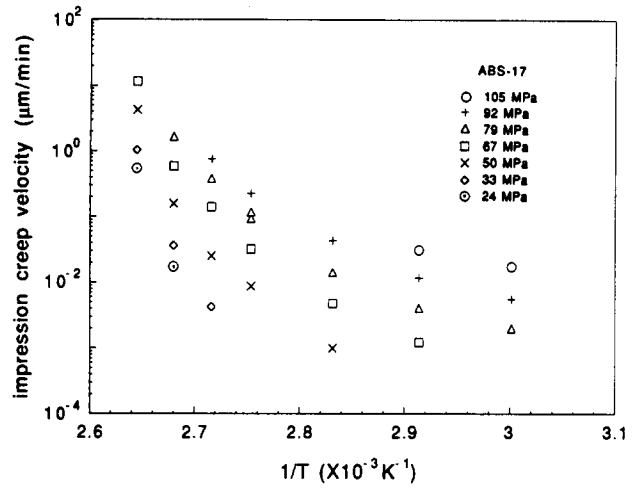

Figure 13 Temperature dependence of the impression velocity for ABS-17

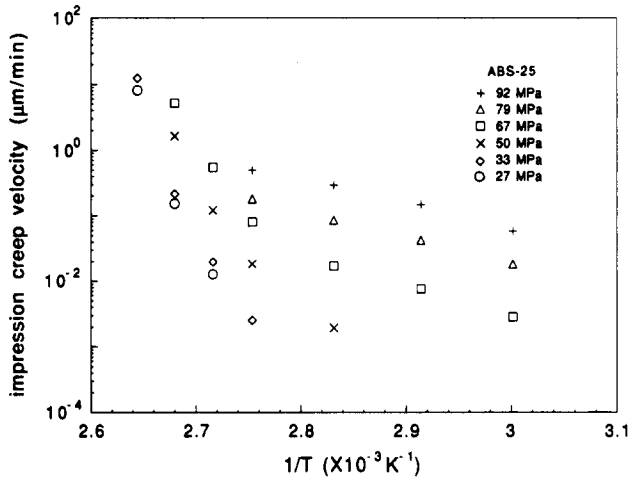

Figure 14 Temperature dependence of the impression velocity for ABS-25

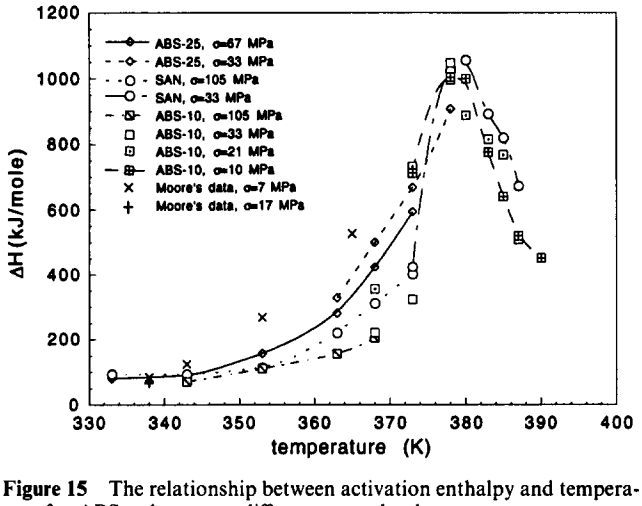

Figure 15 The relationship between activation enthalpy and temperature for ABS polymers at different stress levels

activation enthalpy can be calculated from the slope of each plot. *Figure 15* presents the relationship between the calculated activation enthalpy and temperature. The data obtained from the slopes between the logarithm of the creep rate or viscosity and the reciprocal of absolute temperature by Moore and Gieniewski[4] are shown in the same figure. The stresses shown in the legend are punching stresses in the impression study and tensile stresses in Moore and Gieniewski's data. In general, the applied stress does not have a strong influence on the activation enthalpy at temperatures below 353 K, but the activation enthalpy increases with decreasing stress when the temperature approaches the glass transition temperature. The activation enthalpy for a polymer increases gradually with temperature if the temperature is far below the glass transition temperature. However, the activation enthalpy increases sharply with temperature when the temperature is close to the glass transition temperature but decreases with further increase in temperature above the glass transition. It reaches a maximum around the glass transition temperature.

Sherby and Dorn[16] conducted an experiment to examine the activation enthalpy of poly(methyl methacrylate) (PMMA) as a function of temperature. They measured the strain rate change when a rapid temperature change was imposed on the specimen at a constant load. They found that the activation enthalpy was independent of temperature below 320 K but increased rapidly with increasing temperature after 320 K (320–370 K, $T_g = 373$ K). Tung[17] carried out a constant stress creep test on PMMA and polycarbonate (PC) and found the same tendency for both polymers; namely, the activation enthalpy increased with increasing temperature below T_g and the rate of increase became rapid at temperatures near T_g. Beatty and Weaver[18] performed a compression test and studied the temperature dependences of the modulus, yield stress, percentage yield strain and yield energy for a commercial polystyrene. The relationship between activation enthalpy and temperature had two slopes between 280 K and the glass transition temperature ($T_g \approx 375$ K) with a slope change occurring near the β transition (~ 325 K). The values of the activation enthalpy were 65 kJ mol^{-1} at 280 K, 168 kJ mol^{-1} near the β transition and 480 kJ mol^{-1} near the glass transition. Because of the mechanical instability in the conventional measurements, it is extremely difficult to obtain good data above T_g.

On the other hand, the activation enthalpy of recovery decreases with increasing temperature when the temperature range is above T_g. Andrews[19] conducted retraction measurements on two polystyrene filaments ($T_g \approx 355$ K) with different degrees of orientation. The activation enthalpy decreased from 924 to 546 kJ mol^{-1} for one specimen and from 912 to 487 kJ mol^{-1} for another when the temperature increased from 353 to 368 K. Chang and Li[20] also carried out recovery experiments on compressed atactic polystyrene with a T_g of 373 K. In this case the activation enthalpy decreased with increasing temperature near and above T_g, from 1092 kJ mol^{-1} at 367 K to 529 kJ mol^{-1} at 385 K.

Because creep tends to relax the external stresses imposed on the specimen and recovery relaxes internal stresses inside the specimen, the same mechanisms should be involved in both processes at the same temperature. Tung[17] conducted both creep and recovery experiments below T_g on PMMA and PC in an attempt to correlate the creep and recovery behaviours from the viewpoint of thermally activated processes. After estimating the residual stress inside the specimen during the recovery process, it was found that both the enthalpies determined from recovery and creep at temperatures below T_g for

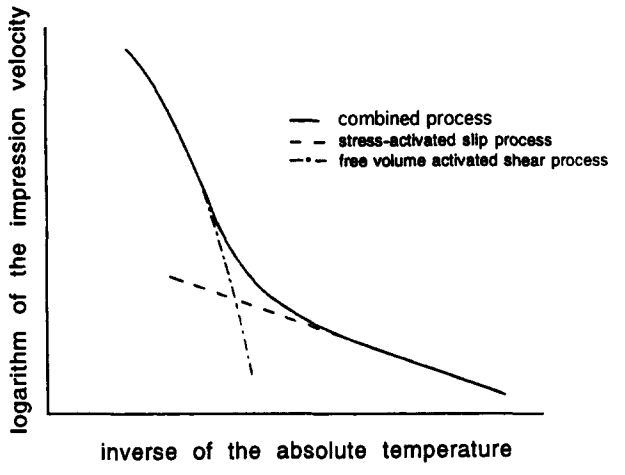

Figure 16 Schematic diagram showing the effect of temperature on impression velocity for two parallel mechanisms in ABS polymers

the two materials were consistent. In view of the experimental results, we believe that the activation enthalpy for deformation of ABS polymers has a maximum value around the glass transition temperature. By using a punch geometry to avoid the mechanical instability in testing, the impression creep method offers a unique way of investigating the creep deformation at temperatures above the glass transition temperature.

Since the volume expansion is faster above the glass transition temperature and a large amount of free volume is added into the material starting at about the glass transition temperature[21], the flow process becomes easier and hence the activation enthalpy decreases after the glass transition temperature. Thereafter, we conclude that the deformation process has two parallel mechanisms. One is a stress-activated slip process which dominates at temperatures below the glass transition temperature, and the other is a free volume activated shear process which dominates at temperatures higher than the glass transition temperature (see *Figure 16*). The way the rate changes with reciprocal temperature (*Figures 11–14*) and the way the activation enthalpy changes with temperature below T_g (*Figure 15*) all point to the possibility of parallel processes[22].

SUMMARY

1. The impression depth–time curves in the impression creep tests of ABS polymers with different butadiene contents resemble the creep curves obtained from the unidirectional tests in that they possess both transient and steady-state stages.
2. The creep resistance of the ABS polymers decreases and the creep rate increases with increasing butadiene content.
3. The impression velocity in the steady-state region is proportional to an exponential function of the applied punching stress. The temperature in the range 333–390 K has little effect on the activation shear strain volume, which increases with increasing butadiene content.
4. The stresses have no strong influence on the activation enthalpy at temperatures below 353 K but the activation enthalpy decreases with increasing stress at higher temperatures.
5. The activation enthalpy increases with temperature gradually at first and then faster in approaching the glass transition temperature. It reaches a maximum of 1050 kJ mol^{-1} at 380 K (T_g = 376 K) and then decreases upon further increase in temperature.
6. Two creep processes appear to take place: one is stress activated and dominates below T_g, and the other is free volume activated and dominates above T_g.

ACKNOWLEDGEMENTS

This work was supported by the NSF through DMR 8819816 and monitored by Dr Bruce MacDonald. We thank Drs David Henton, Charles Lee and C. C. Chau of Dow Chemical Company for supplying the ABS polymers.

REFERENCES

1 Chu, S. N. G. and Li, J. C. M. *Mater. Sci. Eng.* 1979, **39**, 1
2 Gibbs, W. S., Wang. S. H., Matlock, D. K. and Olson, D. L. *Weld. Res. Suppl.* 1985, 153s
3 Yu, E. C. and Li, J. C. M. *Philos. Mag.* 1977, **36**, 811
4 Moore, R. S. and Gieniewski, C. *Macromolecules* 1968, **1**(6), 540
5 Bergen Jr, R. L. and Wolstenholme, W. E. *SPE J.* 1960, 1235
6 Bucknall, C. B. and Drinkwater, I. C. *J. Mater. Sci.* 1973, **8**, 1800
7 Bucknall, C. B. and Reddock, S. E. *J. Mater. Sci.* 1985, **20**, 1434
8 Nielsen, L. E. 'Mechanical Properties of Polymers', Van Nostrand Reinhold, New York, 1962, p. 24
9 Ni, B. Y., Li, J. C. M. and Berry, V. K. *Polymers* 1991, **32**(15), 2766
10 Bucknall, C. B. and Page, C. J. *J. Mater. Sci.* 1982, **17**, 808
11 Li, J. C. M. *Trans. Metall. Soc. AIME* 1965, **233**, 219
12 Meyers, M. A. and Chawla, K. K. 'Mechanical Metallurgy Principles and Applications', Prentice-Hall, Englewood Cliffs, NJ, 1984, p. 612
13 Tabor, D. 'The Hardness of Metals', Clarendon Press, Oxford, 1951, Ch. 3
14 Chu, S. N. G. and Li, J. C. M. *J. Mater. Sci.* 1977, **12**, 2200
15 Li, J. C. M., Pampillo, C. A. and Davis, L. A. 'Deformation and Fracture of High Polymers' (Eds H. H. Kausch, J. A. Hassell and R. I. Jaffee), Plenum Press, New York, 1974, p. 239
16 Sherby, O. D. and Dorn, J. E. *J. Mech. Phys. Solids* 1958, **6**, 145
17 Tung, R. W. PhD dissertation, University of Rochester, New York 1979
18 Beatty, C. L. and Weaver, J. L. *Polym. Eng. Sci.* 1978, **18**(14), 1109
19 Andrews, R. D. *J. Appl. Phys.* 1955, **26**(9), 1061
20 Chang, B. T. A. and Li, J. C. M. *J. Mater. Sci.* 1981, **16**, 889
21 Eisele, U. 'Introduction to Polymer Physics' (Transl. S. D. Pask), Springer, Berlin, 1990, 00. 37–38
22 Li, J. C. M. in 'Rate Processes in Plastic Deformation of Materials' (Eds J. C. M. Li and A. K. Mukherjee), ASM, Materials Park, OH, 1975, pp. 479–496